J. Coat. Technol. Res., **15** (3) 515–526, 2018
https://doi.org/10.1007/s11998-017-0006-7

Effect of acrylation on the properties of waterborne epoxy: evaluation of physicochemical, thermal, mechanical and morphological properties

Sukanya Pradhan, Smita Mohanty, Sanjay K. Nayak

Abstract The present work addresses the critical requirements for the coating industry such as developing the sustainability of biobased materials and simultaneously achieving a balanced combination of coating properties. In this study, acrylated epoxidized soybean oil (AESO) has been successfully synthesized from epoxidized soybean oil and acrylic acid. Subsequently, AESO was modified using a biobased long chain diacid (Pripol-1009) with the assistance of a water/ethanol blend to form waterborne epoxy acrylate (WBEA). The properties of the cured WBEA with 2,5-bis(tert-butylperoxy)-2,5-dimethylhexane as initiator were studied through spectral analysis, coating properties evaluation, corrosion resistance, and morphological and thermal analysis. The results revealed that WBEA exhibited relatively better mechanical, thermal and corrosion resistance characteristics over cured waterborne epoxy.

Keywords Waterborne, Acrylate, Epoxy, Pripol-1009

Introduction

Environmental concern has encouraged research to create a balance between societal, economic and environmental needs. Since the inception of polymer industries in the world, it has always been evolving in a more environmentally friendly direction. In this process of evolution, it has been observed that over the past few decades, biobased resins are in more demand. These polymers are potentially more economical and have less adverse effect on the environment than their petroleum-based counterpart. This is the reason behind the immense interest in using modified plant oils-based epoxy systems as a matrix in the paints and coatings industry. The polymers most sought for the purpose of developing coating and adhesive applications fall in the category of alkyd, polyurethane, epoxy, polyol, polyesteramide, polyetheramide, etc. Epoxy stands out among all the systems, due to its immense potential of adhering to almost all substrates such as metals, concrete, glass, ceramics, leather, etc., that provide effective stability to the coating. But over the past few decades, severe environmental vulnerability has increased due to the utilization of petrobased resins in paint and coatings industry that has triggered the extensive utilization of nontoxic, cheaper and ecofriendly plant oil-based epoxy resins and curing agents owing to their low volatile organic compound (VOC) content, easy cleaning and processability.[1] Waterborne epoxy resin systems are the most preferred polymeric materials for paints and coatings application among other waterborne systems owing to their improved performance like zero VOC, good chemical resistance, low water absorption as well as rapid curing properties. The adopted technique to convert hydrophilic epoxidized plant oils to be more huydrophilic is the inclusion of polar group, viz. carboxyl, amine, anhydride or amide into its hydrophobic backbone.[2] The incorporation of active functional group improves the curing and mechanical properties of the waterborne epoxy coating. In a recent study by Maiorana et al., a plant source-based coating with superior thermal, mechanical properties including high flexibility has been reported which is comparable with that of petroleum-based counterparts.[3] Among all the recently developed waterborne coatings systems, epoxyacrylate-based

S. Pradhan (✉), S. Mohanty, S. K. Nayak
Central Institute of Plastics Engineering and Technology (CIPET), Chennai 600032, India
e-mail: pradhan.sukanya2@gmail.com

S. Mohanty, S. K. Nayak
Laboratory for Advanced Research in Polymeric Materials (LARPM), Bhubaneswar 751024, India

coatings have a greater significance over other systems.[4] The modification of WBE via acrylation is one of the most adopted methods toward achieving the optimum performance characteristics like excellent hardness, chemical resistance and nonyellowing properties. The synthesis of acrylate from epoxidized vegetable oils is due to the opening up of the epoxide group by a ring opening agent that is acrylic acid. A three-dimensional crosslink structure is obtained by the radical and cationic polymerization mechanism of the functional groups of epoxy acrylate.

However, the excess viscosity of the acrylate derived from epoxidized vegetable oils makes it difficult while being implemented in coating applications. Hence, in order to overcome this drawback, a waterborne epoxy acrylate system has been developed. These waterborne polymers have low VOC, and the rapid coating formation ability makes it environment friendly, easy to clean and process, and less toxic. This has made the waterborne coating an efficient ecofriendly coating option which has attracted more attention and can be considered as a promising substitute for VOC producing solventborne polymer coatings.[5] The acrylic groups present in the waterborne epoxy acrylate contributes toward the polymerization via a radical and cationic mechanism, thereby facilitating the formation of three-dimensional networks.[6]

In this study, AESO was synthesized from ESO via incorporating acrylic acid through the controlled reaction and it was further modified with a bioderived diacid. In our previous study, we synthesized waterborne epoxy (WBE) via amination of ESO and it was established that the WBE possessed higher performance characteristics as compared with that of ESO.[7] This study presents a comparative analysis of the properties of WBEA with respect to WBE.

Materials and methods

Materials

ESO was purchased from M/s Makwell Plasticizers Pvt. Ltd, India. Diethanolamine, triethanolamine, 2-methyl imidazole, ethanol and hydroquinone were supplied by M/s Sigma-Aldrich, USA. Acrylic acid and triethylamine (TEA) were purchased from M/s Fischer Scientific, India. Pripol-1009 was kindly supplied by M/s Croda, India.

Synthesis of waterborne epoxy (WBE)

WBE was synthesized as per the process reported in our previous work.[7] In brief, 0.1 mol of ESO was charged into a three-neck round bottom flask equipped with thermometer and magnetic stirrer. 0.1 mol of diethanolamine was slowly added to the reaction system maintained at temperature 50°C with continuous stirring. The temperature of the reaction mixture was gradually raised to 80°C. A solvent blend (50 mL) of ethanol/water in equal proportion was added dropwise to the system, and thus, the designed reddish brown color product of WBE was obtained. The schematic representation of the synthesis of WBE is presented in Fig. 1.

Synthesis of waterborne epoxy acrylate (WBEA)

Fifty grams of ESO, 0.25 g of hydroquinone and 1% of the total weight of the formulation of TEA were charged in a four-neck round bottom flask fitted with reflux condenser, thermometer, mechanical stirrer and a dropping funnel. The system was then heated to 70°C and stirred. Gradually, 8.25 g of acrylic acid was dropped into the reaction system for an hour. The progress of the reaction was observed periodically by measuring the acid value (AV) epoxy equivalent weight (EEW) and viscosity. Then, the reaction temperature was gradually reduced to 60°C. The reaction mixture was cooled down and placed at room temperature for about 1 h. After cooling down to room temperature, the unreacted acrylic acid was removed by dissolving the product in diethyl ether and washed several times with 10% Na_2CO_3 solution. The product was washed with sodium chloride solution and dried over magnesium sulfate. The obtained product was kept in a vacuum oven at 70°C for 4 h to remove diethyl ether. Four drops of triethanolamine were added and stirred slowly to maintain the pH value of the reaction mixture in the range of 6–7, and hence, acrylated ESO was obtained. The reaction of acrylic acid with ESO occurs through a standard substitution and has first-order dependence with respect to epoxy concentration and the second-order dependence with

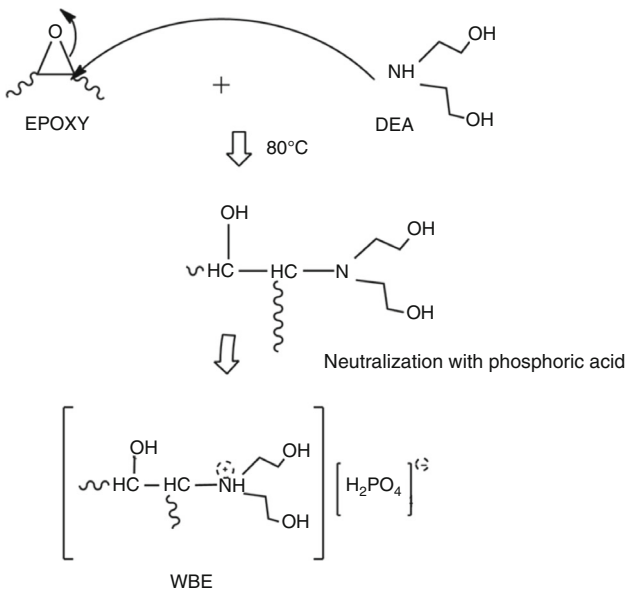

Fig. 1: Schematic representation of synthesis of WBE

respect to acrylic acid concentration. The schematic representation of the mechanism of acrylation is shown in Fig. 2. The obtained AESO contains both unreacted epoxy rings and newly formed hydroxyl groups. Both of these functionalities can be used to further modify the triglyceride. So, the approach presented in the present study was to introduce stiff cyclic rings to the structure by the reaction of AESO with the water-dispersible bioderived diacid (Pripol-1009).

The synthesized AESO was modified with 7.4% of its weight in Pripol-1009 in the presence of 0.1% of its weight in 2-methyl imidazole, as shown in Fig. 3. The reaction was continued for 2 h at 110°C. The modified AESO was mixed with solvent and initiator in the amount of 66 wt% modified AESO, 33 wt% solvent (water/ethanol blend (20v:20v) and 1 wt% 2, 5-bis (tert-butylperoxy)-2, 5-dimethylhexane.

Formulation of coatings

The designed waterborne epoxy acrylate (WBEA) was applied on commercially available mild steel (MS) strips using the drawdown method (ASTM D 4147-93) of thickness 100–110 μm and subjected to curing initially at 65°C for 2 h to avoid the occurrence of any kind of phase separation due to solvent evaporation and then at 120°C for 2 h. For WBE, the prereaction was carried out after mixing by placing it in a vacuum oven at 60°C for 2 h to avoid the occurrence of any kind of phase separation due to solvent evaporation and to obtain a clear and transparent solution. The solution was then poured into a rectangular shaped Teflon mold of dimension 10 cm × 5 cm and subjected to cure initially at 120°C for 2 h and finally at 160°C for 2 h.

Characterization

Physicochemical characteristics

The physicochemical characteristics of ESO and synthesized AESO were investigated by measuring the changes in acid value, gardener color and viscosity.

(a) Acid value (AV)

The acid value was determined as per the titration method with 0.1 N alcoholic KOH solutions as titrant.[8] A blank titration was carried out, and the volume of alkali consumed was recorded. The acid value of all samples was determined according to the following equation (equation (1)).

$$AV = \frac{56.1 \times N \times (A - B)}{W} \quad (1)$$

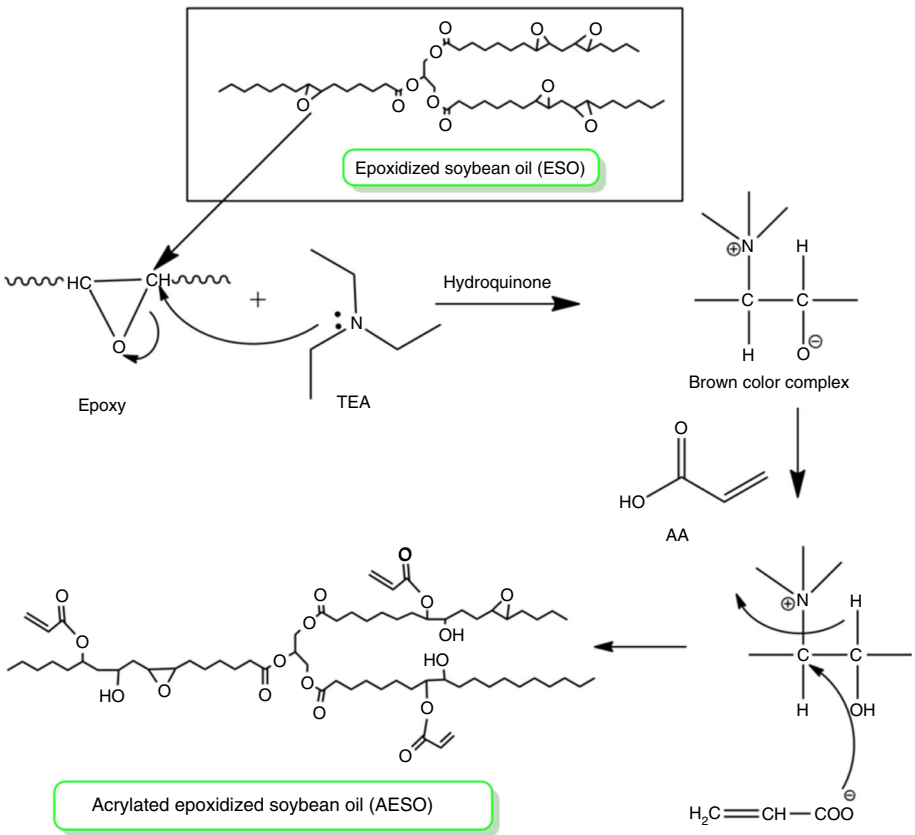

Fig. 2: Mechanism of acrylation of ESO

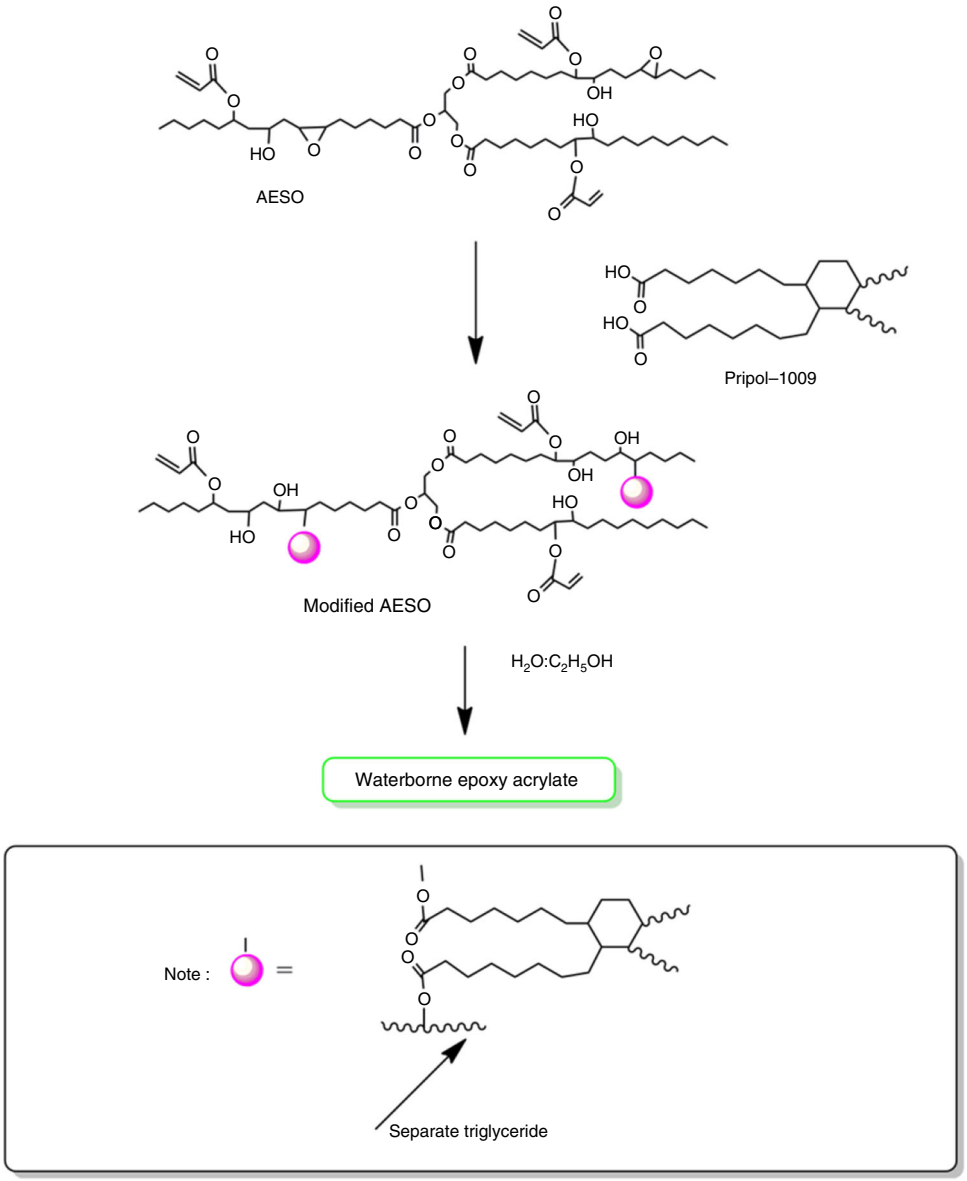

Fig. 3: Modification of AESO

where N = normality of alcoholic KOH, A = burette reading of the sample, B = burette reading of the blank titration, W = weight of the sample.

(b) Viscosity

The viscosity of the samples was determined using Brookfield viscometer with Lv.spindle.3 at room temperature (ASTM D-1824).

Spectral analysis

FTIR-ATR spectra of the samples was recorded using Thermo Scientific FTIR (ATR mode 4000–400 cm^{-1} (M/s Nicolet 6700, USA)) spectrophotometer to investigate the synthesis and curing process.

The proton NMR spectra was recorded for ESO, WBE and AESO using (M/s Bruker 500-NMR, UK) spectrometer with $CDCl_3$ as solvent.

Thermal analysis

The curing profile of uncured WBE and WBEA was examined using DSC Q-20 at a heating rate of 10°C/min under N_2 atmosphere.

The thermal stability of both the samples was characterized using TGA Q 50 v20.13 Build 39 instrument at a heating rate of 10°C/min under

nitrogen atmosphere which ranged from room temperature to 500°C.

Swelling and crosslink density study

The swelling experiments for both WBE and WBEA samples were performed at room temperature as per the procedure reported by Gopalakrishnan and Fernando[9] to calculate the interaction parameter between the solvent used and the polymer and the crosslinking density.

Coating properties

(a) Gloss

The gloss of the coated specimens was evaluated using a glossmeter at a 45° angle in accordance with ASTM D-2457.

(b) Adhesion

The adhesion strength of the coated WBE and WBEA specimens was calculated using the following equation (equation (2)):

$$\text{Adhesion } (\%) = \frac{S_{\text{intact}}}{S_{\text{total}}} \times 100 \tag{2}$$

where S_{intact} = number of squares remained intact to the tape applied area, S_{total} = total number of squares present on the tape applied area.

(c) Scratch hardness

The scratch hardness of five coated MS strips of dimension 70 mm × 25 mm × 1 mm was evaluated using scratch hardness tester with different loads till a clear scratch on the substrate surface was noticed. The average value of five analyses has been reported.

(d) Abrasion resistance

The abrasion resistance of the coated specimens of dimension 10 cm × 10 cm was carried out as per ASTM D 4060 using M/s. Taber Abraser with abrasive wheel No. CS 10 of load 500 g. The weight of the coating material abraded was measured for every 200 cycles of rotation. The test for each sample was run five times, and the average result has been calculated.

(e) Contact angle study

The contact angle study was performed at room temperature using M/s. Phoenix SEO instrument by dropping water on the film surface. For each sample, 5 data were collected and the average contact angle has been reported.

(f) Nanoindentation

The hardness and elastic modulus of the coated specimens were investigated according to Oliver and Pharr method using a UMIS Nanoindentation system (M/s. Frisher-Cripps, Australia) with a Berkovich diamond indenter of tip radius 150 nm, face angle of 63.5 along with a load of 5 mN. For each sample, ten indentations were carried out at different points and the average value was reported. The reduced modulus was determined according to the following equation (equation (3)):

$$E_{\text{r}} = \frac{\sqrt{\pi} S}{2\beta\sqrt{A}} \tag{3}$$

where S = contact stiffness, A = contact area, β = correction factor for the shape of the indenter (=1.07).

The contact area value (A) is obtained from equation (4) by using the calibration function.

$$A = 24.5 h_c^2 \tag{4}$$

h_c^2 = contact depth.

The elastic modulus of the samples (E) is determined by applying the following equation (5)

$$\frac{1}{E_{\text{r}}} = \frac{1 - \nu^2}{E} + \frac{1 - \nu_{\text{i}}^2}{E_{\text{i}}} \tag{5}$$

where E_{r} = reduced modulus, E_{i} = elastic modulus of sample, ν = Poisson's ratio of the sample, ν_{i} = Poisson's ratio of indenter.

(g) Corrosion resistance

The corrosion resistance behaviors of WBE- and WBEA-coated MS substrates of dimension 20 × 10 × 1 mm were studied in different acid and alkali exposure medium for a period of 7 days at room temperature. The corrosion rate (CR) of the bare MS strips and coated WBE, WBEA strips was measured using the following equation (equation (6)):

$$\text{CR} = \frac{KW}{ATD\rho} \tag{6}$$

where W = weight of the sample before exposure − weight of the sample after exposure, A = exposed area of the specimen in square cm, T = total exposure time in hours, ρ = density of the specimen in g/cm^3, K = unit conversion constant (=534).

Another parameter governing the corrosion resistance of the coated specimens is protection efficiency (PE) which was calculated by applying the following equation (equation (7)):

$$\text{PE } (\%) = \frac{\text{CR}_{\text{un}} - \text{CR}_{\text{co}}}{\text{CR}_{\text{un}}} \times 100 \tag{7}$$

where CR_{un} = corrosion resistance of the uncoated specimen, CR_{co} = corrosion resistance of the coated specimen.

Table 1: Physicochemical characteristics of ESO, WBE and AESO

Sample	AV (mg KOH/g)	Viscosity at 25°C (Cp)	Gardener color
ESO	1	474	3
WBE	–	1040	21
AESO	1.5	1675	6

Morphological analysis

Scanning electron microscopy (M/s. EVO MA 15, Germany) was used to study the surface morphology of cured WBE and WBEA. The samples were mounted on the SEM stubs by carbon sticker, sputter coated with gold and the palladium mixture to create a conductive surface layer. After coating, the samples were inserted into SEM instrumental chamber and the morphological micrographs were monitored at an accelerated voltage of 5 kV.

The surface morphology of the samples was recorded in noncontact mode by using AFM (M/s. Park scientific instrument, XE-100, USA) at room temperature.

Results and discussion

Physicochemical characteristics

The physicochemical characteristics of ESO and synthesized AESO and WBEA are displayed in Table 1. An enhancement in the viscosity of WBE was also observed with respect to ESO which can be attributed to the formation of hydroxyl and amide functionalities due to the opening of epoxy rings by the action of diethanolamine. The AESO synthesis process involves the consumption of the carboxylic groups of the acrylic acid and the oxirane rings of ESO. As the acrylation reaction also involves the ring opening of oxirane rings, an increase in viscosity was also observed for AESO. This change reveals the consumption of oxirane rings during the formation of epoxy acrylate. The change in the acid value for AESO was noticed because of the change in concentration of reactive sites and possibility of acid and epoxide groups association.

Proton NMR analysis

The synthesis of WBE and AESO was confirmed through spectral analysis as shown in Figs. 4 and 5. In the case of WBE, the intensity of the peak for oxirane protons at 2.9 ppm was found to be lowered revealing the consumption of oxirane group during the formation of waterborne epoxy. Additionally, a peak at 5.2 ppm was noticed confirming the presence of hydroxyl group formed due to the ring opening of oxirane group. In

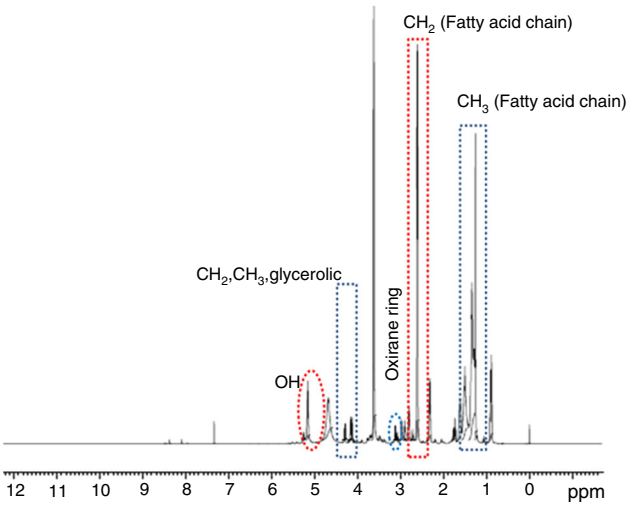

Fig. 4: Proton NMR spectrum of WBE

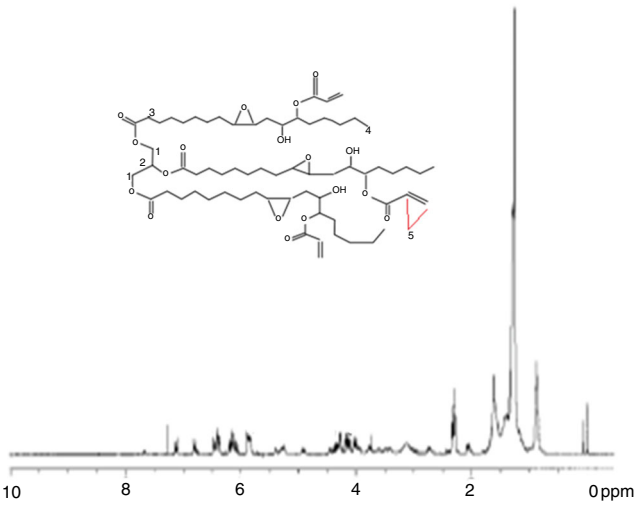

Fig. 5: Proton NMR spectra of AESO

^{1}H-NMR spectrum of AESO, three new signals in the range 5.8–6.5 ppm were noticed on its chain confirming modification after acrylation.[10–12]

Differential scanning calorimetry analysis

The DSC thermogram of uncured WBE and WBEA is depicted in Fig. 6. The curing behavior of the samples was determined as it is the most important step for obtaining samples with good properties. During this curing of WBEA, the interaction between the Pripol and the acrylate and intact epoxy groups occurs. The WBE and WBEA system exhibited heat of reaction values of 268 and 274 J/g, respectively. This shows lower heat of reaction for WBE system due to the fact

that it has fewer crosslinking sites in its structure and fewer crosslinking bonds might have produced as compared to WBEA system. The reaction peak temperature and the heat of reaction are shown in Table 2. The peak temperature around 180 and 240°C was noticed for WBE and WBEA that represents the temperature at which the maximum crosslinking takes place.

Fourier transform infrared spectroscopic (FTIR) analysis

The spectral analysis detail of synthesis of WBE has been reported in our earlier study.[7] The FTIR pattern and curing mechanism of WBE cured with carboxylic groups containing curing agent (Pripol-1009) is presented in Fig. 7. The cured samples of WBE did not show the presence of oxirane peak at 822 cm^{-1} confirming the complete utilization and ring opening of the epoxy rings during curing. The opening of oxirane group occurred via nucleophillic substitution reaction between epoxy and curing agent in the presence of a catalyst. A band at 1560 cm^{-1} was noticed in WBE which can be attributed to the formation of carboxylate intermediate due to the attachment of epoxy resin with the imidazole catalyst. The catalyst might have attacked the carboxylic groups of the curing agent resulting in the formation of carboxylate intermediate that acted as a nucleophile and attacked on the electrophilic carbon, thereby initiating the crosslinking reaction. The nucleophile might attack the oxirane ring or the ester linkage in WBE. However, the carboxylate intermediate attacked the very active oxirane ring due to its high strain. The oxygen present in the oxirane ring served as leaving group that attracted the proton released from curing agent (carboxylic groups), and became protonated. The reaction continued until all oxirane groups were utilized. Moreover, the peak at 1750 cm^{-1} present in uncured WBE was found to have shifted to 1735 cm^{-1} in cured WBE. This showed the formation of new ester linkage due to the interaction between aliphatic ester groups of WBE and carboxylic groups of Pripol. Hence, it can be concluded that both oxirane groups and ester groups act as crosslinking sites in ESO and WBE. In the WBE case, the hydroxyl groups present started to act as crosslinking sites and interacted with the carboxylic end of the remaining curing agent, thereby causing consumption of hydroxyl groups which was confirmed by the absence of peak near 3340 cm^{-1} in cured WBE. This led to the formation of ester, represented by a peak nearly at 1730 cm^{-1} in the case of WBE. The synthesis of WBEA was also analyzed through FTIR analysis and is represented in Fig. 8. The characteristic epoxy absorption band observed at 822 cm^{-1} for neat ESO disappeared completely in the case of WBEA. This suggests the complete utilization of epoxy rings in the formation of WBEA. A new band at 1640 cm^{-1} ascribed to the presence of vinyl moieties (–CH=CH_2) was noticed.[13–15] The curing of WBEA represented in Fig. 8 was monitored by employing FTIR technology. The change in intensities of the characteristic bands for carbon–carbon double bond of the acrylate moieties noticed at 1640 and 814 cm^{-1} was selected to monitor the curing reaction. The absence of a peak at 1640 and 814 cm^{-1} was observed for cured WBEA. This suggests the complete utilization of the acrylate units in the curing process.[16,17]

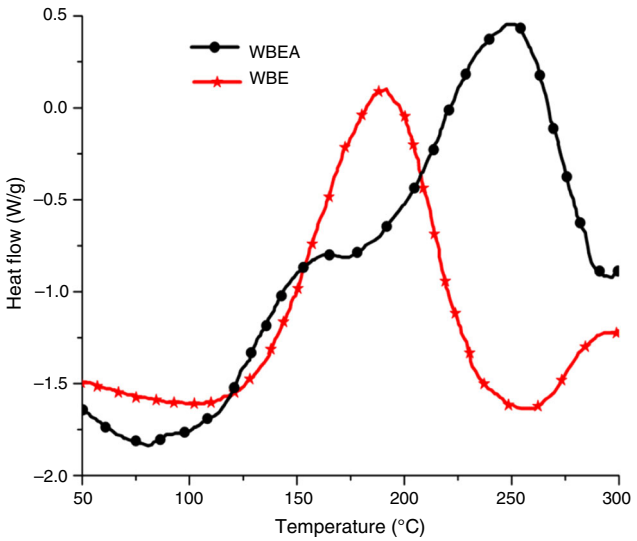

Fig. 6: DSC thermogram of uncured WBE and WBEA

Swelling and crosslink density study

The swelling property of WBE and WBEA were assessed to evaluate their crosslinking and wettability features. The corresponding Gaussian fits of the plots between the swelling coefficient as abscissa and the solubility parameters of the diffusing agents as ordi-

Table 2: Swelling and crosslink density characteristics

Sample	Density (g/cm^3)	S	M_c (g/mol)	Q × 10^{-4} (mol/cm^3)
WBE	0.98	1.39	613	8.16
WBEA	0.99	1.25	530	9.43

nate are depicted in Fig. 9. The results obtained in terms of swelling coefficient (S), crosslink density (Q), average molecular weight between two crosslinks (M_c) are summarized in Table 2. WBE showed higher swelling in all the diffusing media as compared with WBEA. This may be due to the presence of a greater number of crosslinking sites in WBEA that results in a tightly packed structure which in turn inhibits the diffusion of the solvents. Further, the average molecular weight between two crosslinks calculated for WBE was found to be higher than WBEA revealing the highly crosslinked three-dimensional network in WBEA via crosslinking occurred between unsaturation present in acrylate units, remaining oxirane rings, ester groups with the carboxylic ends of pripol. The higher values of crosslinking density obtained for WBEA again revealed the dense crosslink network corroborating the earlier observation.[18] The lower swelling of WBEA in all the media can be attributed to relatively tight packing of crosslinks which does not allow easy penetration of solvent as compared to WBE. This finding resembled the results discussed in previous sections.

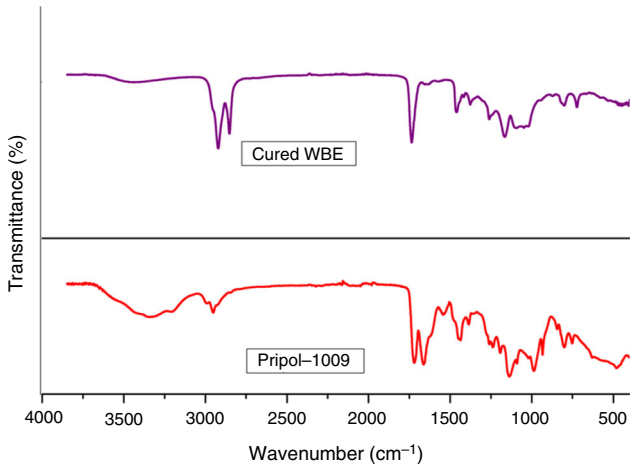

Fig. 7: FTIR spectra of Pripol-1009 and cured WBE

Coating properties

From the results reported in Table 3, it is observed that the WBEA coating showed higher gloss value as compared with WBE which might be due to the development of highly three-dimensional crosslinked network structures in WBEA. The higher adhesive strength in WBEA as compared to WBE indicates its great adhesion performance, which might be attributed to the greater crosslinking density and stronger intermolecular interaction between the epoxy groups, acrylate units with the carboxyl ends of pripol, thereby generating hydrogen bonding.[19] Greater crosslinking and higher H-bonding interactions result in greater adhesive strength. Further, the higher abrasion resistance of WBEA as compared to WBE might be due to effective crosslinking that imparts greater elasticity and resistance against deformation. This suggests that WBEA contains the optimum content of reactive sites that leads to a greater degree of crosslinking.[20] From the results, it can also be observed that the contact angle had increased for WBEA film (77°) as compared to WBE film (70°). This might be due to the effective crosslinking sites in WBEA as observed through FTIR analysis that inhibits the wettability characteristics of the film surface. The scratch hardness of the coatings mainly depends upon the crosslink density. In WBEA acrylate moieties provided effective crosslinking sites when compared that has resulted in enhanced scratch resistance. The nanoindentation results in terms of hardness and elastic modulus showed that WBEA

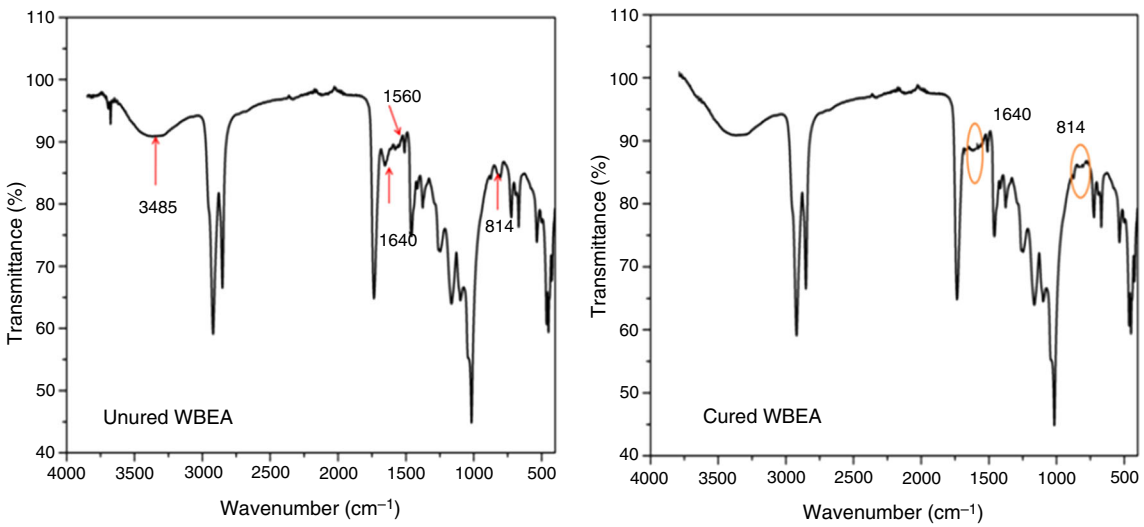

Fig. 8: FTIR spectra of uncured and cured WBEA

exhibited greater hardness and greater elastic modulus value as compared to WBE. This observation can be correlated with the greater crosslinking property of WBEA that has increased the resistance against penetration of the indenter.[21] These observations are found to be consistent with the results obtained from the swelling and crosslinking density experiment discussed in earlier section.

Corrosion resistance

The corrosion resistance behavior of the coated panels in various chemical media like 5 wt% NaCl, 5 wt% HCl, 5 wt% NaOH and distilled water was evaluated by monitoring the changes in weight. From the results of corrosion resistance analysis displayed in Table 4, 5% NaOH was found to be the most corrosive medium for both WBE and WBEA. However, the rate of corrosion of WBEA had the greatest corrosion resistance which was 9.8%, 8.45%, 10.06%, and 23% higher than that of WBE in 5% HCl, 5% NaCl, 5% NaOH and water, respectively. The coatings of WBE and WBEA immersed in 3.5 wt% NaOH solution showed poor resistance that can presumably be ascribed to the presence of ester and ether linkages in the system that are susceptible to alkali attack.[22] Both coatings remained unaffected in water until 30 days of exposure. The lower value of corrosion resistance was noticed for WBE as compared to its counterparts in the entire corrosive medium that might be due to poor crosslinking and adhesion to the substrate,[23] while WBEA showed better performance in every medium owing to its greater crosslinking density and better adherence to the substrate. Further, the higher PE % for WBEA in the entire medium also suggested its greater degree of crosslinking that hindered the penetration of external agents into it.

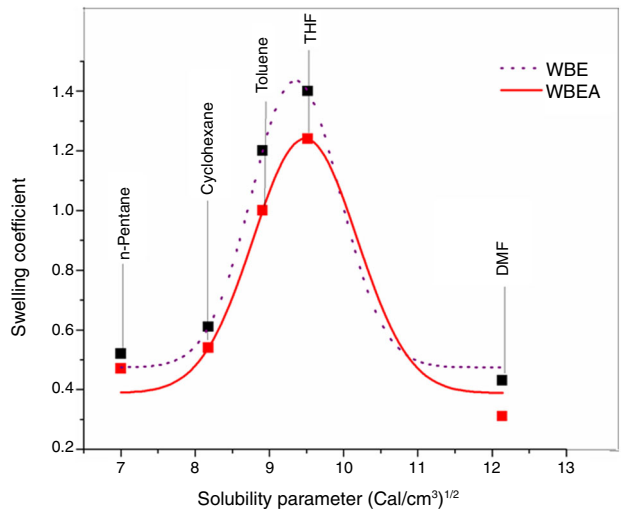

Fig. 9: Gaussian fit for the swelling coefficient vs solubility parameter

Morphological analysis

SEM micrographs of WBE and WBEA shown in Fig. 10 exhibited the surface morphology of the cured film. A uniform surface morphology free of pores and crack defects was observed with no phase separation seen in the case of WBEA that indicated the uniform dispersion of WBEA with pripol. As discussed, the greater reactivity of pripol toward WBEA results in the formation of well-dispersed morphology in case of WBEA/pripol system. However, the SEM micrographs of WBE film surface indicated the appearance of agglomerated structures which might be due to the crystallization and nucleation effect that occurred during the curing process.[24] Further, it is believed that the surface morphology of WBE and WBEA depends solely on the reactivity of the dicarboxylic groups of the curing agent toward the epoxy rings and hydroxyl groups. This concludes that WBEA has a greater reactivity toward pripol that resulted in a higher crosslink network than WBE.

The surface morphology of WBE and WBEA films were further investigated through AFM analysis to ascertain the homogeneity of the cured WBEA system. For WBE, the darker region represents soft segments in ESO moieties while the brighter region corresponds to the hard segments of crosslinker.[25] The presence of dual regions signifies the heterogeneity of the system as shown in Fig. 11. Further, it can be also seen that neither region is uniformly dispersed resulting in noticeable aggregated morphology with dome-shaped structures. However, in the case of WBEA film the

Table 3: Coating properties

Sample	Scratch hardness (g)	Gloss (GU)	Abrasion resistance (mg/1000 cycle)	Adhesion strength (%)	Contact angle (°)	Nanoindentation	
						Hardness (GPa)	Elastic Modulus (GPa)
WBE	1250	52	7.2	61	70	0.45	0.93
WBEA	1550	50	6.3	65	77	0.56	0.98

Table 4: Results of corrosion resistance analysis

Sample	Corrosive medium	CR (g m^2/h)	PE (%)
Uncoated MS	3.5 wt% HCl	13.87	–
WBE coated		2.65	81
WBEA coated		2.39	83
Uncoated MS	3.5 wt% NaCl	5.34	–
WBE coated		0.71	87
WBEA coated		0.65	88
Uncoated MS	3.5 wt% NaOH	14.23	–
WBE coated		4.29	70
WBEA coated		4.77	67
Uncoated MS	Distilled water	5	–
WBE coated		0.56	89
WBEA coated		0.43	91

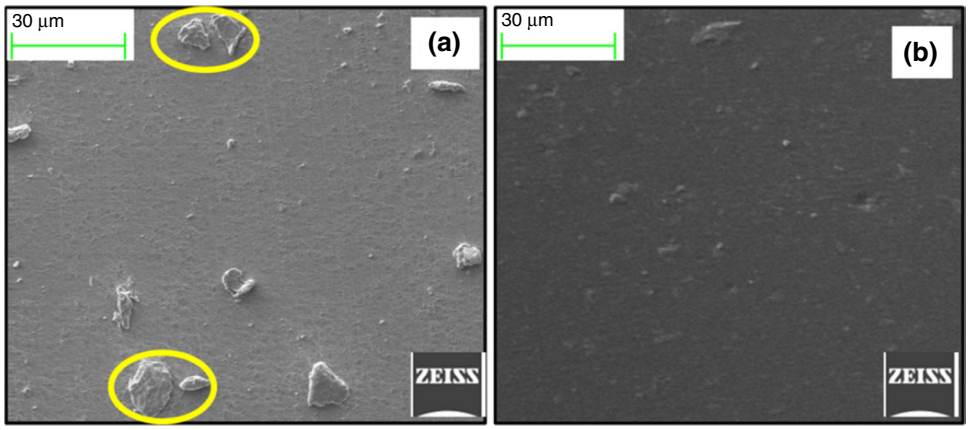

Fig. 10: SEM micrographs of (a) WBE, (b) WBEA

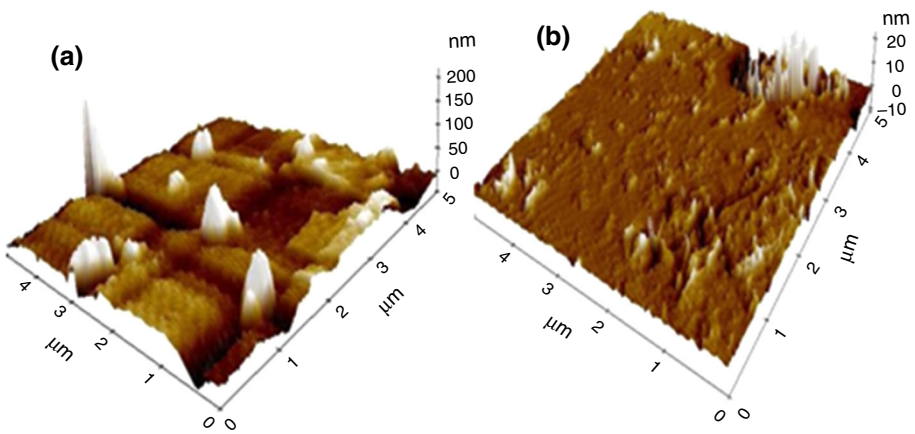

Fig. 11: Noncontact AFM images of (a) WBE, (b) WBEA

absence of any such aggregated structures was noticed. A better surface morphology was obtained for WBEA film as compared to the WBE film which suggests better dispersion and compatibility of WBEA with the crosslinker. The above findings further corroborate with the SEM observations discussed earlier.

Thermogravimetric analysis

Both films exhibited thermal stability up to an elevated temperature of 350°C. However, with further increase in the temperature from 350 to 380°C, the first degradation was observed for WBE and on subsequent

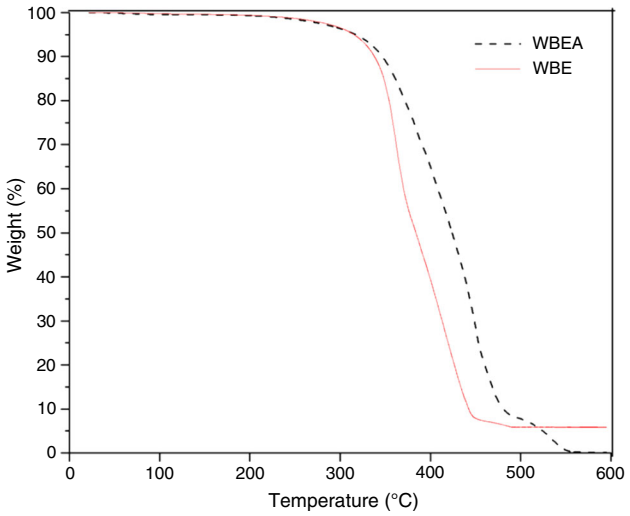

Fig. 12: TGA thermograms of WBE and WBEA

increase in temperature from 380 to 450°C, the second degradation step could be noticed, as shown in Fig. 12. The first degradation attributes to de-crosslinking of WBE and WBEA, while the second decomposition might be due to the decomposition of ester, ether and crosslinker.[26] Beyond 350°C, the first degradation was continued up to 472°C for WBEA while the second step of degradation was noticed in the range 472–548°C. From the TGA thermograms, 3–5% of weight loss was observed for both the samples which can be attributed to the presence of water molecules formed due to reaction between remaining hydroxyl and carboxylic groups. The higher degradation temperature of WBEA revealed the higher thermal stability of WBEA than WBE.

Conclusion

WBEA was synthesized via modification of epoxidized soybean oil (ESO) using acrylic acid as ring opening agent under controlled reaction conditions. WBEA obtained after 3 h of reaction duration was optimized on the basis of the physicochemical properties and FTIR analysis. The proton NMR analysis revealed a successful synthesis of WBEA from ESO. A comparative analysis of WBEA and WBE was carried out on the basis of physico-mechanical properties, corrosion resistance and morphological studies. The FTIR pattern of cured WBEA exhibited the better compatibility with the carboxylic groups of the crosslinker. The higher degree of crosslinking was noticed in case of WBEA as compared with WBE through coating property analysis. Further, the higher PE % for WBEA in all exposure medium also suggested its greater degree of crosslinking that hindered the penetration of external agents into it. The swelling and crosslink density study confirmed higher degree of crosslinking in WBEA. The higher degradation temperature of WBEA revealed the higher thermal stability of WBEA over WBE. On the basis of all results, WBEA was found to be better than WBE in all aspects.

References

1. Pradhan, S, Mohanty, S, Nayak, SK, ''Waterborne Epoxy Adhesive Derived from Epoxidized Soybean Oil and Dextrin: Synthesis and Characterization.'' *Int. J. Polym. Anal. Charact.*, **14** (4) 915–926 (2017)
2. Zafar, S, Riaz, U, Ahmad, S, ''Water-Borne Melamine–Formaldehyde-Cured Epoxy-Acrylate Corrosion Resistant Coatings.'' *J. Appl. Polym. Sci.*, **107** (1) 215–222 (2008)
3. Ma, S, Webster, DC, Jabeen, F, ''Hard and Flexible, Degradable Thermosets from Renewable Bioresources with the Assistance of Water and Ethanol.'' *Macromolecules*, **49** (10) 3780–3788 (2016)
4. Shah, MY, Ahmad, S, ''Waterborne Vegetable Oil Epoxy Coatings: Preparation and Characterization.'' *Prog. Org. Coat.*, **75** 248–252 (2012)
5. Wouters, MEL, Wolfs, DP, Van der Linde, MC, Hovens, JHP, Tinnemans, AHA, ''Transparent UV Curable Antistatic Hybrid Coatings on Polycarbonate Prepared by the Sol–Gel Method.'' *Prog. Org. Coat.*, **51** (4) 312–319 (2004)
6. Wuzella, G, Mahendran, AR, Müller, U, Kandelbauer, A, Teischinger, A, ''Photocrosslinking of an Acrylated Epoxidized Linseed Oil: Kinetics and Its Application for Optimized Wood Coatings.'' *J. Polym. Environ.*, **20** (4) 1063–1074 (2012)
7. Pradhan, S, Pandey, P, Mohanty, S, Nayak, SK, ''Synthesis and Characterization of Waterborne Epoxy Derived from Epoxidized Soybean Oil and Bioderived C-36 Dicarboxylic Acid.'' *J. Coat. Technol. Res.*, (2016). doi:10.1007/s11998-016-9884-3
8. Lenz, RW, ''Experiments in Polymer Science, Edward A. Collins, Jan Bares, Fred W. Billmeyer, Jr., Wiley-Interscience, New York, 1973.'' *J. Polym. Sci. B Polym. Lett. Ed.*, **12** 535–536 (1974)
9. Gopalakrishnan, S, Fernando, TL, ''Bio-Based Thermosetting Tough Polyurethanes.'' *Der. Chem. Sin.*, **2** (5) 54–64 (2011)
10. Salih, AM, Ahmad, MB, Ibrahim, NA, Dahlan, KZHM, Tajau, R, Mahmood, MH, Yunus, WMZW, ''Synthesis of Radiation Curable Palm Oil-Based Epoxy Acrylate: NMR and FTIR Spectroscopic Investigation.'' *Molecules*, **20** (8) 14191–14211 (2015)
11. Habib, F, Bajpai, M, ''Synthesis and Characterization of Acrylated Epoxidized Soybean Oil for UV Cured Coatings.'' *Chem. Chem. Technol.*, **5** (3) 317–326 (2011)
12. Fu, L, Yang, L, Dai, C, Zhao, C, Ma, L, ''Thermal and Mechanical Properties of Acrylated Expoxidized-Soybean Oil-Based Thermosets.'' *J. Appl. Polym. Sci.*, **117** (4) 2220–2225 (2010)
13. Xiao, X, Hao, C, ''Preparation of Waterborne Epoxy Acrylate/Silica Sol Hybrid Materials and Study of Their UV Curing Behavior.'' *Colloids Surf. A Physicochem. Eng. Asp.*, **359** (1) 82–87 (2010)
14. Paluvai, NR, Mohanty, S, Nayak, SK, ''Fabrication and Evaluation of Acrylated Epoxidized Castor Oil-Toughened Diglycidyl Ether of Bisphenol A Nanocomposites.'' *Can. J. Chem. Eng.*, **93** (12) 2107–2116 (2015)

15. Sharmin, E, Ashraf, SM, Ahmad, S, ''Synthesis, Characterization, Antibacterial and Corrosion Protective Properties of Epoxies, Epoxy-Polyols and Epoxy-Polyurethane Coatings from Linseed and Pongamia Glabra Seed Oils.'' *Int. J. Biol. Macromol.*, **40** (5) 407–422 (2007)
16. Gao, J, Lv, H, Zhang, X, Zhao, H, ''Synthesis and Properties of Waterborne Epoxy Acrylate Nanocomposite Coating Modified by MAP-POSS.'' *Prog. Org. Coat.*, **76** (10) 1477–1483 (2013)
17. Ali, MA, Ooi, TL, Salmiah, A, Ishiaku, US, Ishak, ZA, ''New Polyester Acrylate Resins from Palm Oil for Wood Coating Application.'' *J. Appl. Polym. Sci.*, **79** (12) 2156–2163 (2001)
18. Das, S, Pandey, P, Mohanty, S, Nayak, SK, ''Influence of NCO/OH and Transesterified Castor Oil on the Structure and Properties of Polyurethane: Synthesis and Characterization.'' *Mater. Express*, **5** (5) 377–389 (2015)
19. Raj, MM, Patel, HV, Patel, NV, Parmar, JS, ''High Performance Water Borne Coatings from Epoxy Resin and Novel Acrylamide Based Curing Agents.'' *Arch Appl Sci Res*, **6** (3) 35–46 (2014)
20. Hegedus, CR, Pepe, FR, Dickenson, JB, Walker, FH, ''Waterborne Acrylic-Epoxy Coatings.'' *J. Coat. Technol*, **74** (927) 31–39 (2002)
21. Allahverdi, A, Ehsani, M, Janpour, H, Ahmadi, S, ''The Effect of Nanosilica on Mechanical, Thermal and Morphological Properties of Epoxy Coating.'' *Prog. Org. Coat.*, **75** (4) 543–548 (2012)
22. Ma, C, Deng, C, Zheng, W, ''Waterborne Epoxy Resin Modified by AMPS.'' *J. Wuhan Univ. Technol. Mater. Sci. Ed.*, **22** (4) 649–652 (2007)
23. Wegmann, A, ''Chemical Resistance of Waterborne Epoxy/Amine Coatings.'' *Prog. Org. Coat.*, **32** (1) 231–239 (1997)
24. ur Rahman, O, Kashif, M, Ahmad, S, ''Nanoferrite Dispersed Waterborne Epoxy-Acrylate: Anticorrosive Nanocom-
posite Coatings.'' *Prog. Org. Coat.*, **80** 77–86 (2015)
25. Oprea, S, ''Synthesis and Properties of Polyurethane Elastomers with Castor Oil as Crosslinker.'' *J. Am. Oil Chem. Soc.*, **87** (3) 313–320 (2010)
26. Dhoke, SK, Bhandari, R, Khanna, AS, ''Effect of Nano-ZnO Addition on the Silicone-Modified Alkyd-Based Waterborne Coatings on Its Mechanical and Heat-Resistance Properties.'' *Prog. Org. Coat.*, **64** (1) 39–46 (2009)